



STAR: STACKED AUTOREGRESSIVE SCHEME FOR UNIFIED MULTIMODAL LEARNING

Jie Qin * Jiancheng Huang * Limeng Qiao * Lin Ma

Meituan Inc

Project page: <https://star-mm-ai.github.io>

ABSTRACT

Multimodal large language models (MLLMs) play a pivotal role in advancing the quest for general artificial intelligence. However, achieving unified target for multimodal understanding and generation remains challenging due to optimization conflicts and performance trade-offs. To effectively enhance generative performance while preserving existing comprehension capabilities, we introduce *STAR: a S**T**acked Auto**R**egressive scheme for task-progressive unified multimodal learning*. This approach decomposes multimodal learning into multiple stages: understanding, generation, and editing. By freezing the parameters of the fundamental autoregressive (AR) model and progressively stacking isomorphic AR modules, it avoids cross-task interference while expanding the model’s capabilities. Concurrently, we introduce a high-capacity VQ to enhance the granularity of image representations and employ an implicit reasoning mechanism to improve generation quality under complex conditions. Experiments demonstrate that *STAR* achieves state-of-the-art performance on GenEval (**0.91**), DPG-Bench (**87.44**), and ImgEdit (**4.34**), validating its efficacy for unified multimodal learning.

1 INTRODUCTION

In recent years, the rapid advancement of multimodal large language models (MLLMs) has significantly propelled the progress of artificial general intelligence (AGI) (Touvron et al., 2023; Bi et al., 2024; OpenAI, 2024a; Team et al., 2023; DeepSeek-AI et al., 2025; Yang et al., 2025). Numerous studies have focused on constructing unified models that use a single set of parameters to simultaneously handle different tasks, such as multimodal understanding and generation (Wang et al., 2024; Chen et al., 2025c; Wang et al., 2025; Liao et al., 2025; Deng et al., 2025; Xie et al., 2025; OpenAI, 2025; Chen et al., 2025b). However, these from-scratch-trained models face a critical challenge: *inherent conflicts exist between multimodal understanding and generation tasks in both optimization objectives and feature spaces*. This often results in joint training sacrificing performance in one or more domains, thereby limiting the overall capability ceiling of unified models.

Against this backdrop, a fundamental research question emerges: *Can we continuously enhance a model’s image generation capabilities while fully preserving its multimodal understanding abilities?* Existing approaches, such as MetaQuery (Pan et al., 2025) and BLIP3-o (Chen et al., 2025a), adopt a warm-started adaptation paradigm, which initializes from a pre-trained multimodal understanding model and augments it with a diffusion-based generator to enhance generation while preserving image-to-text capability. Yet, these approaches typically require *constructing feature transformation bridges* between autoregressive and diffusion models or *designing complex loss functions*, significantly increasing training complexity. Thus, we face a critical challenge: *How to extend a single MLLM in the most streamlined manner possible, enabling it to progressively acquire more sophisticated multimodal capabilities without compromising existing abilities?*

To address the aforementioned challenge, we propose *STAR (S**T**acked Auto**R**egressive Scheme for Unified Multimodal Learning)*, a novel unified learning method based on stacked autoregressive (AR) paradigm that offers three key design advantages: (i) **a task-progressive training strategy**;

*Equal Contribution.

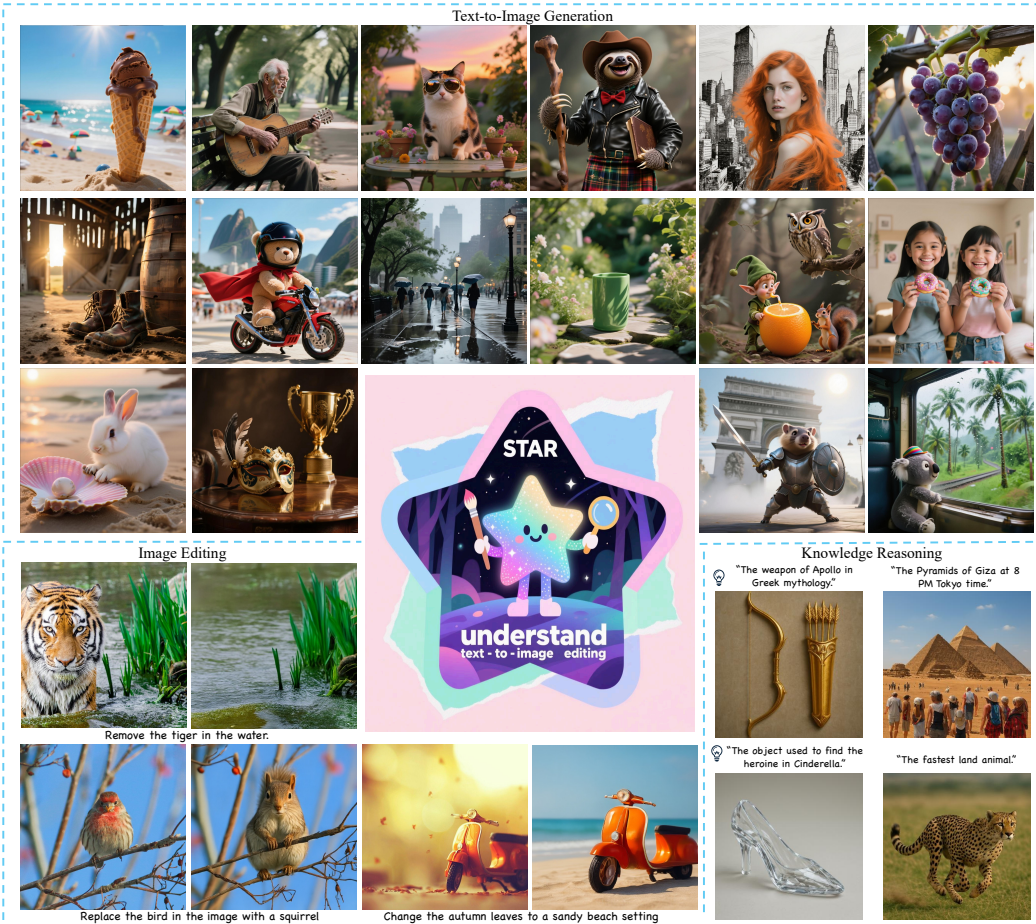


Figure 1: *STAR* enables unified multimodal learning for understanding, text-to-image, image editing, and reasoning, with a diffusion decoder enhancing the granularity of image outputs.

(ii) a **stacked autoregressive model**; and (iii) an **implicit reasoning mechanism**. Firstly, the task-progressive training paradigm decomposes unified multimodal learning into an ordered curriculum: understanding, generation, and editing, while freezing the fundamental AR backbone at each extension. This staged training paradigm simultaneously shields existing comprehension capabilities from catastrophic degradation and equips the model with novel generative abilities. Secondly, the stacked autoregressive model extends the frozen fundamental AR by appending a small set of isomorphic AR modules that share identical architecture and are initialized from the same parameter. The generation and editing tasks can be optimized with the standard next-token prediction objective without any auxiliary adapters or losses. This design is fundamentally distinct from MetaQuery and BLIP3-o, which rely on external bridging modules and diffusion losses. Moreover, instead of learnable queries in MetaQuery, we encode the image as discrete VQ tokens and feed them into the AR model. To furnish the token space with finer granularity, we concurrently introduce a high-capacity vector quantizer from scratch whose codebook contains 65,536 entries of 512-d vectors, termed as *STAR-VQ*. This tokenizer is jointly optimized with a 1B-parameter and is an order of magnitude larger and denser than conventional counterparts, yielding markedly more precise visual tokens that raise the generation ceiling without codebook collapse. Finally, an implicit reasoning mechanism is introduced to harness the stacked architecture at decode time. Given a complex prompt, the fixed AR first performs inference procedure to yield implicit latent tokens, which then serve as conditional input to generate images. By explicitly separating semantic reasoning from pixel generation, this pipeline markedly improves alignment accuracy in challenging compositional and world knowledge scenarios without requiring additional parameters. Qualitative results are presented in the Figure 1.

Extensive experimental results demonstrate that the proposed *STAR* approach not only achieves leading performance across a diverse set of multimodal understanding and generation tasks, but also substantially reduces training complexity through minimal structural modifications. This high-

lights the advantages of progressive task expansion in unified multimodal training. We believe that *STAR* provides an insightful technical pathway toward achieving interference-free, sustainably scalable unified multimodal models. The main contributions of this work can be summarized as follows:

- We propose a task-progressive training paradigm that sequentially learns understanding, generation and editing while freezing the fundamental AR backbone, thereby safeguarding comprehension capabilities against catastrophic degradation.
- We present a stacked-isomorphic AR expansion that appends lightweight, same architecture and initialization modules to the frozen AR model, enabling generation and editing learning with the standard next-token prediction objective and no extra adapters or losses.
- During the inference phase, an implicit reasoning scheme first extracts semantic latent tokens from the frozen understanding AR and utilizes them to generate images, boosting complex-prompt alignment with zero added parameters.
- *STAR* achieves state-of-the-art performance on multimodal benchmarks (e.g., GenEval **0.91**, DPG-Bench **87.44**, ImgEdit **4.34**), validating its efficacy for unified learning.

2 RELATED WORK

Training Unified Multimodal Models from Scratch. Recent efforts toward unified multimodal models typically begin with a pre-trained large language model (LLM) and fine-tune it on paired understanding and image-generation objectives. SEED-X (Ge et al., 2024), Emu (Sun et al., 2023), and MetaMorph (Tong et al., 2024) regress continuous image features. Chameleon (Team, 2024), EMU3 (Wang et al., 2024), and the Janus family (Wu et al., 2024; Chen et al., 2025c) encode images into discrete tokens and unify image and text token prediction under a single next-token prediction objective. DreamLLM (Dong et al., 2023), Show-o (Xie et al., 2024), Show-o2 (Xie et al., 2025), and Transfusion (Zhou et al., 2024) further combine diffusion and next-token losses within one framework. An alternative line appends an external diffusion model after the LLM, like Ovis-U1 (Wang et al., 2025), requires training an intermediate adapter. BAGEL (Deng et al., 2025) and Mogao (Liao et al., 2025) introduce MoE or MoT routers to decouple parameters so that distinct experts handle distinct tasks, while X-Omni (Geng et al., 2025) adds a reinforcement-learning stage to boost generation quality. Despite their effectiveness, these approaches force the backbone to master multiple generation targets, complicating multi-task balancing and motivating our task-progressive alternative.

Training Unified Multimodal Models via Warm-Start Adaptation. An alternative line of research freezes the large multimodal backbone and grafts on lightweight generative modules. LM-Fusion (Shi et al., 2024) trains parallel FFN/QKV experts that share the frozen LLM topology, yet every new backbone necessitates a complete set of newly trained generative parameters, raising computational cost. MetaQuery (Pan et al., 2025) prepends learnable queries to the fixed MLLM and feeds their outputs into a connector that drives a DiT generative model, whereas BLIP3-o (Chen et al., 2025a) directly conditions a diffusion model on MLLM features and supervises the diffusion output with a flow-matching loss against CLIP (Radford et al., 2021) image embeddings. Both approaches require a feature converter to map autoregressive outputs into the diffusion latent space and introduce auxiliary objectives, e.g., diffusion or flow-matching losses, that create optimization paths diverging from the original next-token prediction objective. These shortcomings motivate our stacked-autoregressive task-progressive paradigm, which expands generation capacity while preserving the fundamental comprehension ability.

3 ARCHITECTURE

We introduce *STAR*, as shown in Figure 2, a novel stacked autoregressive scheme for unified multimodal learning that jointly handles visual understanding, text-to-image generation, and image editing within a single framework. Its core components comprise: (i) a vision encoder that maps images into fine-grained tokens; (ii) a stacked autoregressive model that in-place extends isomorphic layers atop a frozen pre-trained vision-language transformer, ensuring rapid convergence with minimal architecture; and (iii) a generative decoder that decodes from discrete tokens, supporting both native

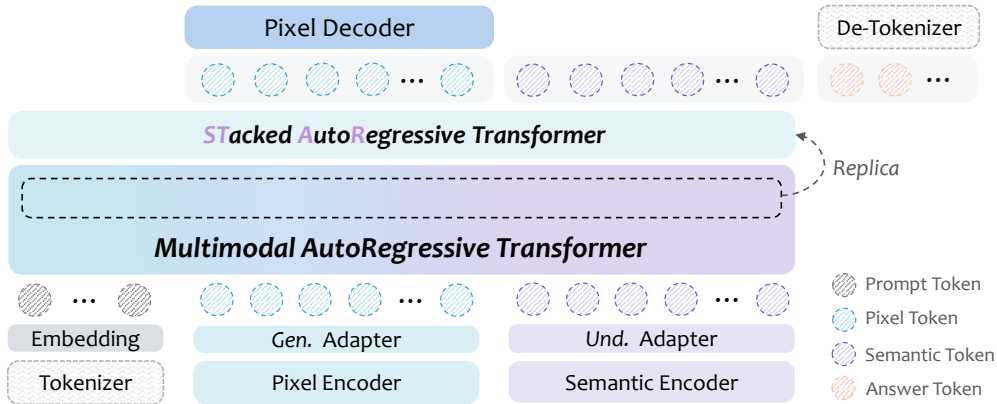


Figure 2: The overall architecture of *STAR*. The architecture integrates two visual encoder (pixel and semantic), a multimodal autoregressive transformer, a stacked autoregressive transformer, and a pixel decoder. The stacked AR is replicated from the last N layer of the multimodal AR.

VQ reconstruction and diffusion-enhanced refinement for improved visual fidelity. The following subsections elaborate on the training procedure of these modules under hybrid-modality objectives.

3.1 VISION ENCODER

For visual input, a unified multimodal model necessitates the simultaneous incorporation of both high-level semantic information and low-level pixel details. To this end, we adopt a dual-decoupled visual representation approach to maximally preserve sufficiently fine-grained visual information for supporting downstream multimodal tasks. On one hand, since *STAR* is warm-started from a well pre-trained multimodal understanding model (Section 3.2), we directly employ the native-resolution continuous visual representations from this model for high-level semantic encoding. These features are flattened from a 2-D feature map into a 1-D token sequence, and an understanding adapter is applied to align the continuous semantic representations with the input space of the following LLM. On the other hand, for low-level pixel representations, we follow the architectural paradigm of VQ-GAN (Esser et al., 2021) and scale the original model in two aspects, proposing a more expressive vector quantizer named *STAR-VQ*. Specifically, the model size is scaled up to $1B$ parameters, with the encoder comprising $0.4B$ parameters and the decoder $0.6B$, while the codebook size and embedding dimension are expanded to $65,536$ and 512 , respectively. After pre-training on a large-scale dataset, the $16\times$ downsampling VQ model achieves image reconstruction quality that rivals that of continuous VAEs. Using the pre-trained *STAR-VQ*, the *STAR* model tokenizes raw images into discrete codebook IDs. A generation adapter is then employed to realign the codebook embeddings corresponding to each ID to the input space of the LLM. Finally, both high-level and low-level representations are concatenated and fed into an autoregressive transformer for deep fusion.

3.2 STACKED AUTOREGRESSIVE MODEL

In this work, we introduce the stacked autoregressive paradigm, a principled approach that converts a pure vision–language understanding model (e.g., Qwen2.5-VL (Bai et al., 2025)) into a unified architecture for comprehension and image generation by stacking additional autoregressive layers upon the base AR transformer, without introducing novel adapters, or external alignment losses. The base multimodal autoregressive transformer remains intact, as each appended layer replicates the self-attention and FFN topology, hidden dimension, and activation function of an existing layer and is initialized by copying that layer’s parameters. Specifically, the parameters of the stacked autoregressive transformer are initialized from the final N layers of the base autoregressive transformer, since these layers are closer to the output and therefore capture higher-level, task-relevant representations. The resulting unified model is expressed as

$$\mathcal{T}_{\text{full}} = \mathcal{T}_{\text{base}} \oplus \mathcal{T}_{\text{stack}}, \tag{1}$$

where $\mathcal{T}_{\text{full}}$ denotes the full autoregressive model, $\mathcal{T}_{\text{base}}$ denotes the frozen base autoregressive transformer, $\mathcal{T}_{\text{stack}}$ denotes the newly appended layers, and \oplus indicates parameter-preserving concatenation along the depth dimension. Consequently, textual, visual, and cross-modal representations

are mapped into a unified feature space, eliminating the 24-layer attentional adaptor used in MetaQuery and the linear projection employed in BLIP3-o and reducing connector-related parameters to exactly zero. This structural homogeneity, coupled with inherited warm-start initialisation, guarantees unimpeded gradient back-propagation and eliminates the feature discrepancy between the autoregressive token space and the continuous noise manifold characteristic of diffusion models. Optimization proceeds under a unified objective: visual inputs are quantized into the discrete token vocabulary, enabling end-to-end training with a single next-token prediction loss,

$$\mathcal{L}_{\text{NTP}} = - \sum_{t=1}^T \log p_{\theta}(x_t | x_{<t}, \mathbf{v}), \quad (2)$$

where x_t denotes the target token at position t , \mathbf{v} denotes the quantized visual tokens, and θ denotes the parameters of the stacked transformer $\mathcal{T}_{\text{full}}$. This obviates the auxiliary diffusion losses required by MetaQuery and the flow-matching objectives with their attendant task-balancing coefficients employed by BLIP3-o, yielding a succinct optimization regime with minimal hyper-parameter overhead. The unified architecture ensures parameter compactness, the consistent feature space guarantees lossless information flow, and the solitary optimisation objective delivers an efficient training regime, collectively improving overall training efficiency.

3.3 GENERATION DECODER

After the stacked AR transformer outputs a sequence of discrete visual tokens, it can be directly fed into the VQ decoder to decode the image. Aiming to enhance both generation quality and super-resolution capability, an additional diffusion model building upon the Lumina2-Image (Qin et al., 2025) framework is proposed to decode images from autoregressively predicted discrete tokens.

For the specific implementation of “AR+Diffusion”, we have established systematic conclusions regarding the types of conditioning and their respective input strategies. Here, the predicted VQ tokens and the target noisy latent are strictly spatially aligned at the pixel level. For low-level tasks where pixel-wise alignment is critical, channel dimension concatenation is the common input strategy (Li et al., 2025). Specifically, let $\mathbf{z}_q \in \mathbb{R}^{K \times d}$ denote the sequence of discrete VQ tokens mapped to feature embeddings, where K is the number of tokens and d the embedding dimension. After reshaping and bilinear resizing we obtain a 2-D feature map $\mathbf{E}_{\text{vq}} \in \mathbb{R}^{h \times w \times d}$ that matches the spatial resolution of the noisy latent $\mathbf{x}_t \in \mathbb{R}^{h \times w \times c}$. The conditioned input to the diffusion transformer, denoted as \mathbf{x}_{in} , is then obtained by channel-wise concatenation:

$$\mathbf{x}_{\text{in}} = \text{concat}[\mathbf{x}_t, \mathbf{E}_{\text{vq}}] \in \mathbb{R}^{h \times w \times (c+d)}, \quad (3)$$

where c is the original latent channel and d is the codebook dimension. The model then performs super-resolution from 384 to 1024 to mitigate token explosion in AR high-resolution generation.

For image editing tasks, the source image VAE latent conditioning is designed to facilitate image consistency. In substantial modifications scenarios, such as removing or adding a large object, spatial alignment between the source image and the target noisy latent may not be strict, making sequence dimension concatenation preferable due to its flexible control over channel concatenation (Huang et al., 2025b; Guo & Lin, 2024). Thus, we choose to concatenate the VAE latent of the source image with the noisy latent along the sequence dimension. Since there is no source image in text-to-image generation, we introduce a zero latent as an unconditional placeholder, allowing joint training of both image editing and text-to-image tasks with a shared diffusion decoder. Consequently, our diffusion decoder accommodates three types of conditioning: text, resized VQ embeddings, and source image VAE latent. Our experimental results consistently validate our theoretical analysis and systematic findings about conditioning strategies.

4 TRAINING AND INFERENCE RECIPE

4.1 TRAINING RECIPE

To achieve multi-stage, incremental enhancement of multi-task capabilities, we adopt a four-stages progressive training framework, whose workflow is illustrated in Figure 3.

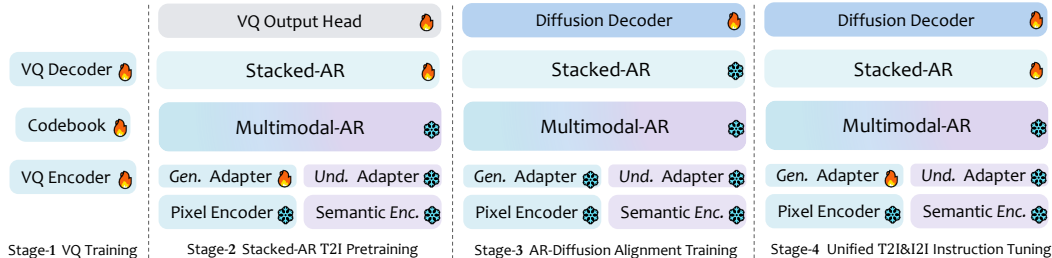


Figure 3: The training stages of *STAR* comprise four task-progressive phases that successively expand capability while preserving all previously acquired skills.

Stage 1: Pixel-level Vector Quantization Pretraining. The objective of this stage is to train a vector quantization model from scratch to achieve a higher-fidelity discrete representation of low-level information of raw images. As introduced in Section 3.1, *STAR-VQ* is designed to reduce quantization information loss by scaling up both model parameter size and codebook dimension. However, such expansion often leads to increased training difficulty and decreased codebook utilization, *i.e.*, codebook collapse. To address this, we draw inspiration from (Chang et al., 2025) and employ an additional codebook projector (2 DiT-blocks) during training, which compresses and reconstructs the codebook, and then performs image reconstruction training based on the reconstructed codebook. This stage involves training on a combined corpus of ImageNet (Deng et al., 2009) and OpenImages (Kuznetsova et al., 2020) for 120 epochs.

Stage 2: Stacked AR Text-to-Image Pretraining. To endow the frozen multimodal backbone with text-to-image generation, we stack isomorphically designed AR layers and train them exclusively on 60M general plus 0.6M high-quality synthetic image-text pairs. The pretrained *STAR-VQ* quantises images into discrete tokens; text and visual tokens are fed to both the base and the stacked AR modules, and next-token cross-entropy loss updates only the newly added parameters, preventing any semantic drift of the original understanding layers.

Stage 3: AR-Diffusion Alignment Training. In this stage, only the diffusion decoder is pre-trained for decoding VQ embeddings, with all other modules frozen and the VQ decoder replaced by the diffusion decoder. Images with a total pixel count close to 512×512 are used, and the training data comprises a 10M-image subset from the text-to-image dataset.

Stage 4: Unified Text-to-Image and Edit Instruction Tuning. In this stage, the diffusion decoder and Stacked-AR are jointly trained on both generation and editing data, aiming to let Stacked-AR impart image editing capabilities while maintaining its text-to-image generation performance. To prevent interference from the diffusion decoder’s loss on Stacked-AR training, a stop-gradient operation is applied when Stacked-AR outputs VQ embeddings. The training data consists of a 6M-image subset from the text-to-image dataset and a 4M-image subset from the editing dataset.

4.2 INFERENCE RECIPE

Upon completion of training, we evaluate the model on three families of tasks: multimodal understanding, text-to-image generation, and image editing, within a single forward pipeline. For understanding, the frozen base autoregressive transformer receives an image-text question and directly emits the textual answer. For generation, the text prompt is processed sequentially by the base and the stacked AR layers, which progressively predict the discrete image-token sequence. The resulting tokens are fed to the generative decoder to reconstruct a image. For editing, the original image and the textual instruction are concatenated and processed by the stacked AR model, yielding an edited token sequence that is decoded into a semantically consistent result. When the prompt demands external knowledge or complex reasoning, we invoke an *implicit-token-reasoning* mechanism: the base AR first infers an intermediate latent-token sequence that encodes the required knowledge, and this sequence is supplied as an conditioning signal to the stacked AR for image generation. Experiments show that this strategy yields substantial gains on generation benchmarks that probe world knowledge and compositional semantics.

Table 1: Evaluation on multimodal understanding benchmarks.

Model	#LLM	MMB	MMStar	MathVista	SEED	MME-P	MMMU	OCRBench	POPE	DocVQA
Seed-X (Ge et al., 2024)	13B	70.1	-	-	66.5	1457.0	35.6	-	-	-
EMU3 (Wang et al., 2024)	8B	58.5	-	-	68.2	1243.8	31.6	68.7	85.2	-
MetaMorph (Tong et al., 2024)	8B	75.2	-	-	71.8	-	41.8	-	-	-
Janus (Wu et al., 2024)	1.3B	75.5	-	-	63.7	1338.0	30.5	-	87.0	-
Janus-Pro (Chen et al., 2025c)	7B	79.2	87.4	-	72.1	1567.1	41.0	-	-	-
BLIP3-o (Chen et al., 2025a)	8B	83.5	-	-	77.5	1682.6	50.6	-	-	-
Show-o2 (Xie et al., 2025)	7B	79.3	56.6	-	69.8	1620.0	48.9	-	-	-
MetaQuery-XL (Pan et al., 2025)	7B	83.5	-	-	76.9	1685.2	58.6	-	-	-
Bagel (Deng et al., 2025)	14B	85.0	-	73.1	-	1687.0	55.3	-	-	-
Ovis-U1 (Wang et al., 2025)	1.5B	77.8	-	69.4	-	-	51.1	88.3	-	-
ILLUME+ (Huang et al., 2025a)	3B	80.8	-	-	73.3	1414.0	44.3	67.2	87.6	80.8
X-Omni (Geng et al., 2025)	7B	74.8	-	-	74.1	-	-	70.4	89.3	88.6
STAR-3B	3B	80.1	55.8	62.3	74.0	1592.3	53.1	79.7	85.9	93.9
STAR-7B	7B	83.9	63.9	68.1	77.0	1690.1	58.6	86.4	86.6	95.7

5 EXPERIMENT

5.1 DATA COMPOSITION

Text-to-Image Generation Data. This dataset is primarily used for training text-to-image generation tasks. We collected publicly available text-image pairs and leveraged powerful generative models such as FLUX (Labs, 2024), GPT-4o (OpenAI, 2025), and Midjourney. Ultimately, we constructed a total of 60M text-to-image generation data.

Image Edit Data. In our experiments, we utilize a diverse set of pre-trained image editing datasets to support both the Stage-3 and Stage-4 training. The publicly available image editing data comprises main sources from UltraEdit (Zhao et al., 2024), HQ-Edit (Hui et al., 2024), and Omni-Edit (Wei et al., 2024), approximately 4M samples are selected. Also, we re-synthesized ground truth images using the GPT-4o (OpenAI, 2025) on approximately 300K proprietary samples. This combination of large-scale public and private datasets, along with high-fidelity ground truth synthesis, ensures robust and comprehensive supervision for image editing task throughout training.

5.2 EVALUATION SETUP

Image Understanding Evaluation. We assess image-understanding capabilities on the nine standardized benchmarks: MMBench-EN (Liu et al., 2023), MMStar (Chen et al., 2024), MathVista (Lu et al., 2023), SEEDBench (Li et al., 2023), MME (Fu et al., 2023), MMMU (Yue et al., 2024), OCRBench (Liu et al., 2024), POPE (Yifan et al., 2023), and DocVQA (Mathew et al., 2021).

Text-to-image Evaluation. This task evaluates semantic consistency on GenEval (Ghosh et al., 2023) (553 prompts) and DPG-Bench (Hu et al., 2024) (1065 prompts), and world knowledge is measured on WISEBench (Niu et al., 2025) (1000 prompts).

Image Editing Evaluation. Image-editing capability is assessed on MagicBrush (Zhang et al., 2023) (1,000 pairs) and ImgEdit (Ye et al., 2025) (737 pairs), the latter covering object-level, background, style, action, and composite manipulations. For MagicBrush we report CLIP-I, DINO (content preservation), and L1 (pixel-level fidelity).

5.3 MAIN RESULTS

Image Understanding. Thanks to our task-progressive training regime, the proposed model family can be grafted onto any state-of-the-art multimodal understanding backbone without impairing its original capability. By freezing the comprehension parameters and augmenting capacity through stacked autoregressive modules, we retain the full representational strength of the upstream encoder while equipping it with high-fidelity generation. Consequently, our checkpoints inherit both the semantic richness of the underlying understanding network and the generative power of contemporary SOTA architectures. As shown in Table 1, they achieve competitive or leading results on a broad range of understanding benchmarks, including MMStar, SEED, MME and OCRBench,

Table 2: Comparison with state-of-the-art text-to-image generation methods on GenEval (Ghosh et al., 2023) and DPG-Bench (Hu et al., 2024).

Method	GenEval						DPG-Bench						
	Single	Two	Count.	Colors	Pos.	Color Attr.	Overall	Global	Entity	Attr.	Relation	Other	Overall
<i>Gen. Only Models</i>													
SDXL (Podell et al., 2024)	0.98	0.74	0.39	0.85	0.15	0.23	0.55	83.27	82.43	80.91	86.76	80.41	74.65
DALL-E (OpenAI, 2024b)	0.96	0.87	0.47	0.83	0.43	0.45	0.67	90.97	89.61	88.39	90.58	89.83	83.50
SD3-medium (Esser et al., 2024)	0.99	0.94	0.72	0.89	0.33	0.60	0.74	87.90	91.01	88.83	80.70	88.68	84.08
FLUX.1-dev (Labs, 2024)	0.98	0.93	0.75	0.93	0.68	0.65	0.82	82.10	89.50	88.70	91.10	89.40	84.00
OmniGen2 (Wu et al., 2025)	0.99	0.96	0.74	0.98	0.72	0.75	0.86	88.81	88.83	90.18	89.37	90.27	83.57
<i>Unified Models</i>													
Emu3 (Wang et al., 2024)	0.99	0.81	0.42	0.80	0.49	0.45	0.66	85.21	86.68	86.84	90.22	83.15	80.60
ILLUME+ (Huang et al., 2025a)	0.99	0.88	0.62	0.84	0.42	0.53	0.72	-	-	-	-	-	-
Janus-Pro (Chen et al., 2025c)	0.99	0.89	0.59	0.90	0.79	0.66	0.80	86.90	88.90	89.40	89.32	89.48	84.19
MetaQuery (Pan et al., 2025)	-	-	-	-	-	-	0.80	-	-	-	-	-	82.05
BLIP3-o (Chen et al., 2025a)	-	-	-	-	-	-	0.84	-	-	-	-	-	81.60
UniWorld-V1 (Lin et al., 2025)	0.99	0.93	0.81	0.89	0.74	0.71	0.84	83.64	88.39	88.44	89.27	87.22	81.38
Mogao (Liao et al., 2025)	1.00	0.97	0.83	0.93	0.84	0.80	0.89	82.37	90.03	88.26	93.18	85.40	84.33
BAGEL (Deng et al., 2025)	0.98	0.95	0.84	0.95	0.78	0.77	0.88	88.94	90.37	91.29	90.82	88.67	85.07
Show-o2 (Xie et al., 2025)	1.00	0.87	0.58	0.92	0.52	0.62	0.76	89.00	91.78	89.96	91.81	91.64	86.14
GPT-4o (OpenAI, 2025)	0.99	0.92	0.85	0.92	0.75	0.61	0.84	82.27	91.27	87.67	93.85	88.71	86.23
X-Omni (Geng et al., 2025)	0.98	0.95	0.75	0.91	0.71	0.68	0.83	84.80	92.59	90.63	94.75	84.20	87.65
Ovis-U1 (Wang et al., 2025)	0.98	0.98	0.90	0.92	0.79	0.75	0.89	82.37	90.08	88.68	93.35	85.20	83.72
STAR-3B	0.98	0.87	0.85	0.91	0.79	0.76	0.86	93.00	90.49	91.71	90.72	92.75	87.30
STAR-7B	0.98	0.94	0.90	0.92	0.91	0.80	0.91	94.97	92.91	91.62	94.30	83.82	87.44

Table 3: Comparison of world knowledge reasoning on WISE (Niu et al., 2025).

Methods	Cultural	Time	Space	Biology	Physics	Chemistry	Overall
<i>Gen. Only Models</i>							
SD-XL (Podell et al., 2024)	0.43	0.48	0.47	0.44	0.45	0.27	0.43
SD-3.5-large (Esser et al., 2024)	0.44	0.50	0.58	0.44	0.52	0.31	0.46
FLUX.1-dev (Labs, 2024)	0.48	0.58	0.62	0.42	0.51	0.35	0.50
<i>Unified Models</i>							
Emu3 (Wang et al., 2024)	0.34	0.45	0.48	0.41	0.45	0.27	0.39
Janus-Pro-7B (Chen et al., 2025c)	0.30	0.37	0.49	0.36	0.42	0.26	0.35
MetaQuery-XL (Pan et al., 2025)	0.56	0.55	0.62	0.49	0.63	0.41	0.55
BLIP3-o (Chen et al., 2025a)	-	-	-	-	-	-	0.62
BAGEL (Deng et al., 2025)	0.76	0.69	0.75	0.65	0.75	0.58	0.70
GPT-4o (OpenAI, 2025)	0.94	0.64	0.98	0.93	0.98	0.95	0.89
STAR-3B	0.58	0.54	0.48	0.49	0.51	0.54	0.52
STAR-7B	0.61	0.67	0.61	0.74	0.69	0.66	0.66

demonstrating that task-progressive extension yields a unified system that excels simultaneously in comprehension and generation.

Image Generation. We comprehensively evaluated the generative capability of our model on three public benchmarks: GenEval and DPG-Bench for prompt-image alignment, and WISE for world-knowledge reasoning. For the latter, we further activated the proposed implicit-reasoning pipeline at inference to mitigate visual-semantic distributional shifts. As reported in Table 2, the model establishes a new state-of-the-art on GenEval with 0.91 (2.0% over the prior best Ovis-U1), while delivering competitive scores on DPG-Bench in Table 2. As shown in the Table 3, implicit inference reasoning on WISE (Niu et al., 2025) attains a score of 0.66, confirming that latent-token mediation significantly enhances compositional and knowledge-intensive generation as shown in Figure 4.

Image Editing. Tables 4 and 5 present the evaluation results for image editing capabilities on MagicBrush and ImgEdit, respectively. On ImgEdit, we compare our model with existing unified models. For the MagicBrush, in addition to unified models, we also include comparisons with specialized image editing models such as Instruct-Pix2Pix, UltraEdit (Zhao et al., 2024), and ICEdit. The performance of previous models on ImgEdit is referenced from Ovis-u1, while the MagicBrush results are computed by us. Overall, our model achieves strong performance across both benchmarks.

5.4 ABLATION STUDIES

Different type of VQ tokenizer. To obtain higher-fidelity discrete image representations, we replaced the conventional VQGAN reconstruction tokenizer with the STAR-VQ. Table 6a compares

Table 4: Comparison of image editing performance on the MagicBrush (Zhang et al., 2023).

	MagicBrush	Instruct-Pix2Pix	UltraEdit	ICedit	OmniGen	UniReal	BAGEL	STAR-3B	STAR-7B
L1 ↓	0.074	0.114	0.066	0.060	0.116	0.081	0.074	0.056	0.060
CLIP-I ↑	0.908	0.851	0.904	0.928	0.863	0.903	0.914	0.934	0.931
DINO ↑	0.847	0.744	0.852	0.853	0.821	0.837	0.827	0.857	0.853

Table 5: Comparison of image editing performance on ImgEdit-Bench (Ye et al., 2025).

Model	Add	Adjust	Extract	Replace	Remove	Background	Style	Hybrid	Action	Overall
<i>Edit. Only Models</i>										
MagicBrush (Zhang et al., 2023)	2.84	1.58	1.51	1.97	1.58	1.75	2.38	1.62	1.22	1.90
Instruct-Pix2Pix (Brooks et al., 2023)	2.45	1.83	1.44	2.01	1.50	1.44	3.55	1.20	1.46	1.88
AnyEdit (Yu et al., 2025)	3.18	2.95	1.88	2.47	2.23	2.24	2.85	1.56	2.65	2.45
UltraEdit (Zhao et al., 2024)	3.44	2.81	2.13	2.96	1.45	2.83	3.76	1.91	2.98	2.70
Step1X-Edit (Liu et al., 2025)	3.88	3.14	1.76	3.40	2.41	3.16	4.63	2.64	2.52	3.06
ICedit (Zhang et al., 2025)	3.58	3.39	1.73	3.15	2.93	3.08	3.84	2.04	3.68	3.05
<i>Unified Models</i>										
GPT-4o (OpenAI, 2025)	4.61	4.33	2.90	4.35	3.66	4.57	4.93	3.96	4.89	4.20
OmniGen (Xiao et al., 2024)	3.47	3.04	1.71	2.94	2.43	3.21	4.19	2.24	3.38	2.96
BAGEL (Deng et al., 2025)	3.56	3.31	1.70	3.30	2.62	3.24	4.49	2.38	4.17	3.20
UniWorld-V1 (Lin et al., 2025)	3.82	3.64	2.27	3.47	3.24	2.99	4.21	2.96	2.74	3.26
OmniGen2 (Wu et al., 2025)	3.57	3.06	1.77	3.74	3.20	3.57	4.81	2.52	4.68	3.44
Ovis-U1 (Wang et al., 2025)	4.13	3.62	2.98	4.45	4.06	4.22	4.69	3.45	4.61	4.00
STAR-3B	4.26	4.06	3.78	4.46	4.34	4.19	4.53	3.29	4.38	4.14
STAR-7B	4.33	4.19	4.19	4.59	4.58	4.36	4.59	3.67	4.60	4.34



Figure 4: (a) Qualitative comparison results. The proposed diffusion decoder yields sharper textures and finer details than the VQ decoder, demonstrating its superior high-fidelity generation capability. (b) Reasoning mode can utilize the world knowledge of MLLM for reasoning-based text-to-image.

the two approaches under a controlled 3B architecture trained on 6M synthetic images and evaluated on GenEval. **STAR-VQ** raises the GenEval score from 0.414 to 0.439, confirming that its larger and higher-dimensional codebook yields finer-grained visual tokens. The gain indicates that the augmented discrete vocabulary supplies the autoregressive generator with more precise spatial and semantic cues, ultimately translating into superior synthesis quality.

The number of layers in the stacked AR. To identify the optimal depth of the stacked autoregressive transformer, we perform layer-wise ablation on the **STAR-3B** model trained with 6M data and evaluated on GenEval. As reported in Table 6b, accuracy increases with depth until 16 layers, which attains the highest score of 0.439, and declines thereafter. This inverted-U profile indicates that shallow stacks lack the capacity to model the target distribution, whereas deeper model suffer from diminishing gradient signals that progressively weaken updates and ultimately degrade performance.

The initialization strategy of stacked AR. To determine the optimal initialization for the stacked autoregressive modules, we train **STAR-3B** model on 6 M generation data and evaluate on GenEval. As shown in Table 6c, VLM-based initialization reaches 0.439, exceeding LLM-based initialization (0.403) and random initialization (0.374), respectively. Initializing stacked AR layers with parameters homologous to the primary AR leverages strong inherent feature-space alignment, thereby accelerating convergence and enhancing generation quality by eliminating re-alignment and directly exploiting learned representational priors.

Table 6: Ablation studies of VQ and stacked AR.

(a) Different type of VQ tokenizer. Size and Dim represent the code-book size and dimension of token.				(b) The number of layers.		(c) Ablation of initial of stacked AR.	
VQ Type	Size	Dim	GenEval	Layer	GenEval	Init From	GenEval
VQGAN	16384	8	0.414	8	0.347	Rand	0.374
STAR-VQ	65536	512	0.439	16	0.439	LLM	0.403
				32	0.410	VLM	0.439
				36	0.394		

Table 7: Ablation studies of diffusion decoder.

(a) The impact of the diffusion decoder.				(b) The input way from AR to DiT.	
Stage	Decoder Type	Size	GenEval	Input of VQ emb	GenEval
Stage 3	VQ Dec.	384	0.723	Text-wise Concat	0.703
Stage 3	Diffusion	1024	0.756	Sequence-wise Concat	0.712
Stage 4	VQ Dec.	384	0.858	Channel-wise Concat	0.756
Stage 4	Diffusion	1024	0.868		

The impact of Diffusion decoder. To elucidate the role of the diffusion decoder in autoregressive text-to-image generation, we replace the vanilla VQ decoder with a diffusion decoder. As reported in Table 7a, the switch yields consistent gains on GenEval (0.03 at stage3 and 0.01 at stage4), corroborating that iterative denoising recovers high-frequency information lost during quantization. Qualitative visualizations in Figure 4 further reveal markedly sharper textures, cleaner edges and suppressed aliasing artifacts, validating that the diffusion translates coarse AR tokens into photo-realistic outputs with enhanced pixel fidelity.

The input strategy of Diffusion decoder. We ablate three strategies for feeding AR tokens into the diffusion decoder: (i) text-wise concatenation; (ii) sequence-wise concatenation; and (iii) channel-wise concatenation after resizing. They are trained on a subset of the dataset. Table 7b shows that strategy channel-wise concatenation after resizing achieves the highest GenEval score (0.756), establishing it as the preferred interface.

6 CONCLUSION

In this work, we present **STAR**, a task-progressive framework that unifies multimodal understanding, generation, and editing within a single MLLM without sacrificing any capability. By freezing the original autoregressive model and incrementally stacking isomorphic AR layers, **STAR** eliminates cross-task gradient interference. We further equip the generative AR with **STAR-VQ**, a high-capacity tokenizer that boosts discrete-image fidelity, and an implicit inference mechanism that leverages intermediate semantic tokens to handle complex prompts. Extensive experiments show that **STAR** sets new state-of-the-art results on both comprehension and generation tasks. These findings validate that orderly, interference-free expansion is a viable route toward scalable and sustainable general-purpose multimodal systems.

REFERENCES

Shuai Bai, Keqin Chen, Xuejing Liu, Jialin Wang, Wenbin Ge, Sibao Song, Kai Dang, Peng Wang, Shijie Wang, Jun Tang, Humen Zhong, Yuanzhi Zhu, Mingkun Yang, Zhaohai Li, Jianqiang Wan, Pengfei Wang, Wei Ding, Zheren Fu, Yiheng Xu, Jiabo Ye, Xi Zhang, Tianbao Xie, Zesen Cheng, Hang Zhang, Zhibo Yang, Haiyang Xu, and Junyang Lin. Qwen2.5-vl technical report. *arXiv preprint arXiv:2502.13923*, 2025.

Xiao Bi, Deli Chen, Guanting Chen, Shanhuang Chen, Damai Dai, Chengqi Deng, Honghui Ding, Kai Dong, Qiushi Du, Zhe Fu, et al. Deepseek llm: Scaling open-source language models with longtermism. *arXiv preprint arXiv:2401.02954*, 2024.

Tim Brooks, Aleksander Holynski, and Alexei A Efros. Instructpix2pix: Learning to follow image editing instructions. In *Proceedings of the IEEE/CVF conference on computer vision and pattern recognition*, pp. 18392–18402, 2023.

- Yifan Chang, Jie Qin, Limeng Qiao, Xiaofeng Wang, Zheng Zhu, Lin Ma, and Xingang Wang. Scalable training for vector-quantized networks with 100% codebook utilization. *arXiv preprint arXiv:2509.10140*, 2025.
- Jiuhai Chen, Zhiyang Xu, Xichen Pan, Yushi Hu, Can Qin, Tom Goldstein, Lifu Huang, Tianyi Zhou, Saining Xie, Silvio Savarese, et al. Blip3-o: A family of fully open unified multimodal models-architecture, training and dataset. *arXiv preprint arXiv:2505.09568*, 2025a.
- Lin Chen, Jinsong Li, Xiaoyi Dong, Pan Zhang, Yuhang Zang, Zehui Chen, Haodong Duan, Jiaqi Wang, Yu Qiao, Dahua Lin, et al. Are we on the right way for evaluating large vision-language models? *Advances in Neural Information Processing Systems*, 37:27056–27087, 2024.
- Sixiang Chen, Jinbin Bai, Zhuoran Zhao, Tian Ye, Qingyu Shi, Donghao Zhou, Wenhao Chai, Xin Lin, Jianzong Wu, Chao Tang, et al. An empirical study of gpt-4o image generation capabilities. *arXiv preprint arXiv:2504.05979*, 2025b.
- Xiaokang Chen, Zhiyu Wu, Xingchao Liu, Zizheng Pan, Wen Liu, Zhenda Xie, Xingkai Yu, and Chong Ruan. Janus-pro: Unified multimodal understanding and generation with data and model scaling. *arXiv preprint arXiv:2501.17811*, 2025c.
- DeepSeek-AI, Aixin Liu, Bei Feng, Bing Xue, Bingxuan Wang, Bochao Wu, Chengda Lu, Cheng-gang Zhao, Chengqi Deng, Chenyu Zhang, and et al. Deepseek-v3 technical report, 2025. URL <https://arxiv.org/abs/2412.19437>.
- Chaorui Deng, Deyao Zhu, Kunchang Li, Chenhui Gou, Feng Li, Zeyu Wang, Shu Zhong, Weihao Yu, Xiaonan Nie, Ziang Song, Guang Shi, and Haoqi Fan. Emerging properties in unified multimodal pretraining. *arXiv preprint arXiv:2505.14683*, 2025.
- Jia Deng, Wei Dong, Richard Socher, Li-Jia Li, Kai Li, and Li Fei-Fei. Imagenet: A large-scale hierarchical image database. In *2009 IEEE conference on computer vision and pattern recognition*, pp. 248–255. Ieee, 2009.
- Runpei Dong, Chunrui Han, Yuang Peng, Zekun Qi, Zheng Ge, Jinrong Yang, Liang Zhao, Jianjian Sun, Hongyu Zhou, Haoran Wei, et al. Dreamllm: Synergistic multimodal comprehension and creation. *arXiv preprint arXiv:2309.11499*, 2023.
- Patrick Esser, Robin Rombach, and Bjorn Ommer. Taming transformers for high-resolution image synthesis. In *Proceedings of the IEEE/CVF conference on computer vision and pattern recognition*, pp. 12873–12883, 2021.
- Patrick Esser, Sumith Kulal, Andreas Blattmann, Rahim Entezari, Jonas Müller, Harry Saini, Yam Levi, Dominik Lorenz, Axel Sauer, Frederic Boesel, et al. Scaling rectified flow transformers for high-resolution image synthesis. In *Forty-first international conference on machine learning*, 2024.
- Chaoyou Fu, Peixian Chen, Yunhang Shen, Yulei Qin, Mengdan Zhang, Xu Lin, Jinrui Yang, Xiawu Zheng, Ke Li, Xing Sun, Yunsheng Wu, and Rongrong Ji. Mme: A comprehensive evaluation benchmark for multimodal large language models. *arXiv preprint arXiv:2306.13394*, 2023.
- Yuying Ge, Sijie Zhao, Jinguo Zhu, Yixiao Ge, Kun Yi, Lin Song, Chen Li, Xiaohan Ding, and Ying Shan. Seed-x: Multimodal models with unified multi-granularity comprehension and generation. *arXiv preprint arXiv:2404.14396*, 2024.
- Zigang Geng, Yibing Wang, Yeyao Ma, Chen Li, Yongming Rao, Shuyang Gu, Zhao Zhong, Qinglin Lu, Han Hu, Xiaosong Zhang, et al. X-omni: Reinforcement learning makes discrete autoregressive image generative models great again. *arXiv preprint arXiv:2507.22058*, 2025.
- Dhruba Ghosh, Hannaneh Hajishirzi, and Ludwig Schmidt. Geneval: An object-focused framework for evaluating text-to-image alignment. *Advances in Neural Information Processing Systems*, 36: 52132–52152, 2023.
- Qin Guo and Tianwei Lin. Focus on your instruction: Fine-grained and multi-instruction image editing by attention modulation. In *Proceedings of the IEEE/CVF Conference on Computer Vision and Pattern Recognition*, pp. 6986–6996, 2024.

- Xiwei Hu, Rui Wang, Yixiao Fang, Bin Fu, Pei Cheng, and Gang Yu. Ella: Equip diffusion models with llm for enhanced semantic alignment. *CoRR*, 2024.
- Runhui Huang, Chunwei Wang, Junwei Yang, Guansong Lu, Yunlong Yuan, Jianhua Han, Lu Hou, Wei Zhang, Lanqing Hong, Hengshuang Zhao, et al. Illume+: Illuminating unified mllm with dual visual tokenization and diffusion refinement. *arXiv preprint arXiv:2504.01934*, 2025a.
- Yi Huang, Jiancheng Huang, Yifan Liu, Mingfu Yan, Jiayi Lv, Jianzhuang Liu, Wei Xiong, He Zhang, Liangliang Cao, and Shifeng Chen. Diffusion model-based image editing: A survey. *IEEE Transactions on Pattern Analysis and Machine Intelligence*, 2025b.
- Mude Hui, Siwei Yang, Bingchen Zhao, Yichun Shi, Heng Wang, Peng Wang, Yuyin Zhou, and Cihang Xie. Hq-edit: A high-quality dataset for instruction-based image editing. *arXiv preprint arXiv:2404.09990*, 2024.
- Alina Kuznetsova, Hassan Rom, Neil Alldrin, Jasper Uijlings, Ivan Krasin, Jordi Pont-Tuset, Shahab Kamali, Stefan Popov, Matteo Mallocci, Alexander Kolesnikov, et al. The open images dataset v4: Unified image classification, object detection, and visual relationship detection at scale. *International journal of computer vision*, 128(7):1956–1981, 2020.
- Black Forest Labs. Flux. <https://github.com/black-forest-labs/flux>, 2024.
- Bohao Li, Rui Wang, Guangzhi Wang, Yuying Ge, Yixiao Ge, and Ying Shan. Seed-bench: Benchmarking multimodal llms with generative comprehension. *arXiv preprint arXiv:2307.16125*, 2023.
- Xin Li, Yulin Ren, Xin Jin, Cuiling Lan, Xingrui Wang, Wenjun Zeng, Xinchao Wang, and Zhibo Chen. Diffusion models for image restoration and enhancement: a comprehensive survey. *International Journal of Computer Vision*, pp. 1–31, 2025.
- Chao Liao, Liyang Liu, Xun Wang, Zhengxiong Luo, Xinyu Zhang, Wenliang Zhao, Jie Wu, Liang Li, Zhi Tian, and Weilin Huang. Mogao: An omni foundation model for interleaved multi-modal generation. *arXiv preprint arXiv:2505.05472*, 2025.
- Bin Lin, Zongjian Li, Xinhua Cheng, Yuwei Niu, Yang Ye, Xianyi He, Shenghai Yuan, Wangbo Yu, Shaodong Wang, Yunyang Ge, et al. Uniworld: High-resolution semantic encoders for unified visual understanding and generation. *arXiv preprint arXiv:2506.03147*, 2025.
- Shiyu Liu, Yucheng Han, Peng Xing, Fukun Yin, Rui Wang, Wei Cheng, Jiaqi Liao, Yingming Wang, Honghao Fu, Chunrui Han, et al. Step1x-edit: A practical framework for general image editing. *arXiv preprint arXiv:2504.17761*, 2025.
- Yuan Liu, Haodong Duan, Yuanhan Zhang, Bo Li, Songyang Zhang, Wangbo Zhao, Yike Yuan, Jiaqi Wang, Conghui He, Ziwei Liu, et al. Mmbench: Is your multi-modal model an all-around player? *arXiv preprint arXiv:2307.06281*, 2023.
- Yuliang Liu, Zhang Li, Mingxin Huang, Biao Yang, Wenwen Yu, Chunyuan Li, Xu-Cheng Yin, Cheng-Lin Liu, Lianwen Jin, and Xiang Bai. Ocrbench: on the hidden mystery of ocr in large multimodal models. *Science China Information Sciences*, 67(12):220102, 2024.
- Pan Lu, Hritik Bansal, Tony Xia, Jiacheng Liu, Chunyuan Li, Hannaneh Hajishirzi, Hao Cheng, Kai-Wei Chang, Michel Galley, and Jianfeng Gao. Mathvista: Evaluating mathematical reasoning of foundation models in visual contexts. *arXiv preprint arXiv:2310.02255*, 2023.
- Minesh Mathew, Dimosthenis Karatzas, and CV Jawahar. Docvqa: A dataset for vqa on document images. In *Proceedings of the IEEE/CVF winter conference on applications of computer vision*, pp. 2200–2209, 2021.
- Yuwei Niu, Munan Ning, Mengren Zheng, Weiyang Jin, Bin Lin, Peng Jin, Jiaqi Liao, Chaoran Feng, Kunpeng Ning, Bin Zhu, et al. Wise: A world knowledge-informed semantic evaluation for text-to-image generation. *arXiv preprint arXiv:2503.07265*, 2025.
- OpenAI. Hello gpt-4o, 2024a. URL <https://openai.com/index/hello-gpt-4o>.

- OpenAI. Dall-e 3. <https://openai.com/index/dall-e-3/>, 2024b.
- OpenAI. Addendum to gpt-4o system card: 4o image generation, 2025. Accessed: April 2, 2025.
- Xichen Pan, Satya Narayan Shukla, Aashu Singh, Zhuokai Zhao, Shlok Kumar Mishra, Jialiang Wang, Zhiyang Xu, Jiuhai Chen, Kunpeng Li, Felix Juefei-Xu, et al. Transfer between modalities with metaqueries. *arXiv preprint arXiv:2504.06256*, 2025.
- Dustin Podell, Zion English, Kyle Lacey, Andreas Blattmann, Tim Dockhorn, Jonas Müller, Joe Penna, and Robin Rombach. Sdxl: Improving latent diffusion models for high-resolution image synthesis. In *The Twelfth International Conference on Learning Representations*, 2024.
- Qi Qin, Le Zhuo, Yi Xin, Ruoyi Du, Zhen Li, Bin Fu, Yiting Lu, Jiakang Yuan, Xinyue Li, Dongyang Liu, et al. Lumina-image 2.0: A unified and efficient image generative framework. *arXiv preprint arXiv:2503.21758*, 2025.
- Alec Radford, Jong Wook Kim, Chris Hallacy, Aditya Ramesh, Gabriel Goh, Sandhini Agarwal, Girish Sastry, Amanda Askell, Pamela Mishkin, Jack Clark, et al. Learning transferable visual models from natural language supervision. In *ICML*, pp. 8748–8763, 2021.
- Weijia Shi, Xiaochuang Han, Chunting Zhou, Weixin Liang, Xi Victoria Lin, Luke Zettlemoyer, and Lili Yu. Lmfusion: Adapting pretrained language models for multimodal generation. *arXiv preprint arXiv:2412.15188*, 2024.
- Quan Sun, Qiyang Yu, Yufeng Cui, Fan Zhang, Xiaosong Zhang, Yueze Wang, Hongcheng Gao, Jingjing Liu, Tiejun Huang, and Xinlong Wang. Generative pretraining in multimodality. *arXiv:2307.05222*, 2023.
- Chameleon Team. Chameleon: Mixed-modal early-fusion foundation models. *arXiv preprint arXiv:2405.09818*, 2024.
- Gemini Team, Rohan Anil, Sebastian Borgeaud, Yonghui Wu, Jean-Baptiste Alayrac, Jiahui Yu, Radu Soricut, Johan Schalkwyk, Andrew M Dai, Anja Hauth, et al. Gemini: a family of highly capable multimodal models. *arXiv preprint arXiv:2312.11805*, 2023.
- Shengbang Tong, David Fan, Jiachen Zhu, Yunyang Xiong, Xinlei Chen, Koustuv Sinha, Michael Rabbat, Yann LeCun, Saining Xie, and Zhuang Liu. Metamorph: Multimodal understanding and generation via instruction tuning. *arXiv preprint arXiv:2412.14164*, 2024.
- Hugo Touvron, Thibaut Lavril, Gautier Izacard, Xavier Martinet, Marie-Anne Lachaux, Timothée Lacroix, Baptiste Rozière, Naman Goyal, Eric Hambro, Faisal Azhar, et al. Llama: Open and efficient foundation language models. *arXiv preprint arXiv:2302.13971*, 2023.
- Guo-Hua Wang, Shanshan Zhao, Xinjie Zhang, Liangfu Cao, Pengxin Zhan, Lunhao Duan, Shiyin Lu, Minghao Fu, Jianshan Zhao, Yang Li, and Qing-Guo Chen. Ovis-u1 technical report. *arXiv preprint arXiv:2506.23044*, 2025.
- Xinlong Wang, Xiaosong Zhang, Zhengxiong Luo, Quan Sun, Yufeng Cui, Jinsheng Wang, Fan Zhang, Yueze Wang, Zhen Li, Qiyang Yu, et al. Emu3: Next-token prediction is all you need. *arXiv preprint arXiv:2409.18869*, 2024.
- Cong Wei, Zheyang Xiong, Weiming Ren, Xinrun Du, Ge Zhang, and Wenhui Chen. Omniedit: Building image editing generalist models through specialist supervision. *arXiv preprint arXiv:2411.07199*, 2024.
- Chengyue Wu, Xiaokang Chen, Zhiyu Wu, Yiyang Ma, Xingchao Liu, Zizheng Pan, Wen Liu, Zhenda Xie, Xingkai Yu, Chong Ruan, et al. Janus: Decoupling visual encoding for unified multimodal understanding and generation. *arXiv preprint arXiv:2410.13848*, 2024.
- Chenyuan Wu, Pengfei Zheng, Ruiran Yan, Shitao Xiao, Xin Luo, Yueze Wang, Wanli Li, Xiyan Jiang, Yexin Liu, Junjie Zhou, Ze Liu, Ziyi Xia, Chaofan Li, Haoge Deng, Jiahao Wang, Kun Luo, Bo Zhang, Defu Lian, Xinlong Wang, Zhongyuan Wang, Tiejun Huang, and Zheng Liu. Omnigen2: Exploration to advanced multimodal generation. *arXiv preprint arXiv:2506.18871*, 2025.

- Shitao Xiao, Yueze Wang, Junjie Zhou, Huaying Yuan, Xingrun Xing, Ruiran Yan, Shuting Wang, Tiejun Huang, and Zheng Liu. Omnigen: Unified image generation. *arXiv preprint arXiv:2409.11340*, 2024.
- Jinheng Xie, Weijia Mao, Zechen Bai, David Junhao Zhang, Weihao Wang, Kevin Qinghong Lin, Yuchao Gu, Zhijie Chen, Zhenheng Yang, and Mike Zheng Shou. Show-o: One single transformer to unify multimodal understanding and generation. *arXiv preprint arXiv:2408.12528*, 2024.
- Jinheng Xie, Zhenheng Yang, and Mike Zheng Shou. Show-o2: Improved native unified multimodal models. *arXiv preprint arXiv:2506.15564*, 2025.
- An Yang, Anfeng Li, Baosong Yang, Beichen Zhang, Binyuan Hui, Bo Zheng, Bowen Yu, Chang Gao, Chengen Huang, Chenxu Lv, Chujie Zheng, Dayiheng Liu, Fan Zhou, Fei Huang, Feng Hu, Hao Ge, Haoran Wei, Huan Lin, Jialong Tang, Jian Yang, Jianhong Tu, Jianwei Zhang, Jianxin Yang, Jiayi Yang, Jing Zhou, Jingren Zhou, Junyang Lin, Kai Dang, Keqin Bao, Kexin Yang, Le Yu, Lianghao Deng, Mei Li, Mingfeng Xue, Mingze Li, Pei Zhang, Peng Wang, Qin Zhu, Rui Men, Ruize Gao, Shixuan Liu, Shuang Luo, Tianhao Li, Tianyi Tang, Wenbiao Yin, Xingzhang Ren, Xinyu Wang, Xinyu Zhang, Xuancheng Ren, Yang Fan, Yang Su, Yichang Zhang, Yinger Zhang, Yu Wan, Yuqiong Liu, Zekun Wang, Zeyu Cui, Zhenru Zhang, Zhipeng Zhou, and Zihan Qiu. Qwen3 technical report, 2025. URL <https://arxiv.org/abs/2505.09388>.
- Yang Ye, Xianyi He, Zongjian Li, Bin Lin, Shenghai Yuan, Zhiyuan Yan, Bohan Hou, and Li Yuan. Imgedit: A unified image editing dataset and benchmark. *arXiv preprint arXiv:2505.20275*, 2025.
- Li Yifan, Du Yifan, Zhou Kun, Wang Jinpeng, XinZhao Wayne, and Wen Ji-Rong. Evaluating object hallucination in large vision-language models. In *The 2023 Conference on Empirical Methods in Natural Language Processing*, 2023. URL <https://openreview.net/forum?id=xozJw0kZXF>.
- Qifan Yu, Wei Chow, Zhongqi Yue, Kaihang Pan, Yang Wu, Xiaoyang Wan, Juncheng Li, Siliang Tang, Hanwang Zhang, and Yueting Zhuang. Anyedit: Mastering unified high-quality image editing for any idea. In *Proceedings of the Computer Vision and Pattern Recognition Conference*, pp. 26125–26135, 2025.
- Xiang Yue, Yuansheng Ni, Kai Zhang, Tianyu Zheng, Ruoqi Liu, Ge Zhang, Samuel Stevens, Dongfu Jiang, Weiming Ren, Yuxuan Sun, et al. Mmmu: A massive multi-discipline multi-modal understanding and reasoning benchmark for expert agi. In *Proceedings of the IEEE/CVF Conference on Computer Vision and Pattern Recognition*, pp. 9556–9567, 2024.
- Kai Zhang, Lingbo Mo, Wenhui Chen, Huan Sun, and Yu Su. Magicbrush: A manually annotated dataset for instruction-guided image editing. *Advances in Neural Information Processing Systems*, 36:31428–31449, 2023.
- Zechuan Zhang, Ji Xie, Yu Lu, Zongxin Yang, and Yi Yang. In-context edit: Enabling instructional image editing with in-context generation in large scale diffusion transformer. *arXiv preprint arXiv:2504.20690*, 2025.
- Haozhe Zhao, Xiaojian Shawn Ma, Liang Chen, Shuzheng Si, Rujie Wu, Kaikai An, Peiyu Yu, Minjia Zhang, Qing Li, and Baobao Chang. Ultraedit: Instruction-based fine-grained image editing at scale. *Advances in Neural Information Processing Systems*, 37:3058–3093, 2024.
- Chunting Zhou, Lili Yu, Arun Babu, Kushal Tirumala, Michihiro Yasunaga, Leonid Shamis, Jacob Kahn, Xuezhe Ma, Luke Zettlemoyer, and Omer Levy. Transfusion: Predict the next token and diffuse images with one multi-modal model. *arXiv preprint arXiv:2408.11039*, 2024.

A OVERALL ARCHITECTURAL PARAMETERS

Overall architectural parameters are summarised in Table 8, confirming the compactness of the proposed design. *STAR-3B* extends the Qwen2.5-VL-3B (Bai et al., 2025) vision–language model by appending a Stacked AR module that replicates the final 16 layers of the VLM for initialization, contributing 1.5 B additional parameters. *STAR-7B*, built upon Qwen2.5-VL-7B (Bai et al., 2025), mirrors the last 14 layers of the VLM, adding 3 B parameters. Both variants share an identical VQ tokenizer and diffusion decoder.

Table 8: Overall architecture constituents and parameter counts.

Model	VLM	Pixel-Enc.	Gen-Adapter	Stacked-AR	VQ-Dec.	Diff-Dec.
<i>STAR-3B</i>	Qwen2.5-VL-3B	0.4B	5M	1.2B (16 Layer)	0.6B	2.6B
<i>STAR-7B</i>	Qwen2.5-VL-7B	0.4B	38M	3B (14 Layer)	0.6B	2.6B

B TRAINING STRATEGIES AT EACH STAGE

We also list the training strategies we used in each stage in Table 9.

Table 9: Training strategies at each stage.

Hyper-Parameter	Stage 1	Stage 2	Stage 3	Stage 4
Learning Rate	1e-4	1e-3	1e-4	1e-3
LR Scheduler	cosine	constant	constant	constant
Optimizer	AdamW	Adamw	AdamW	AdamW
Batch Size	256	4096	2048	4608
Training Steps	1406K	20K	4K	8K
VQ Image Res.	256×256	384×384	384×384	384×384
Diffusion Res.	/	/	512×512	1024×1024

C MORE QUALITATIVE RESULTS

We give more qualitative results on text-to-image generation (Figure 5 and 6) and image-editing (Figure 7).

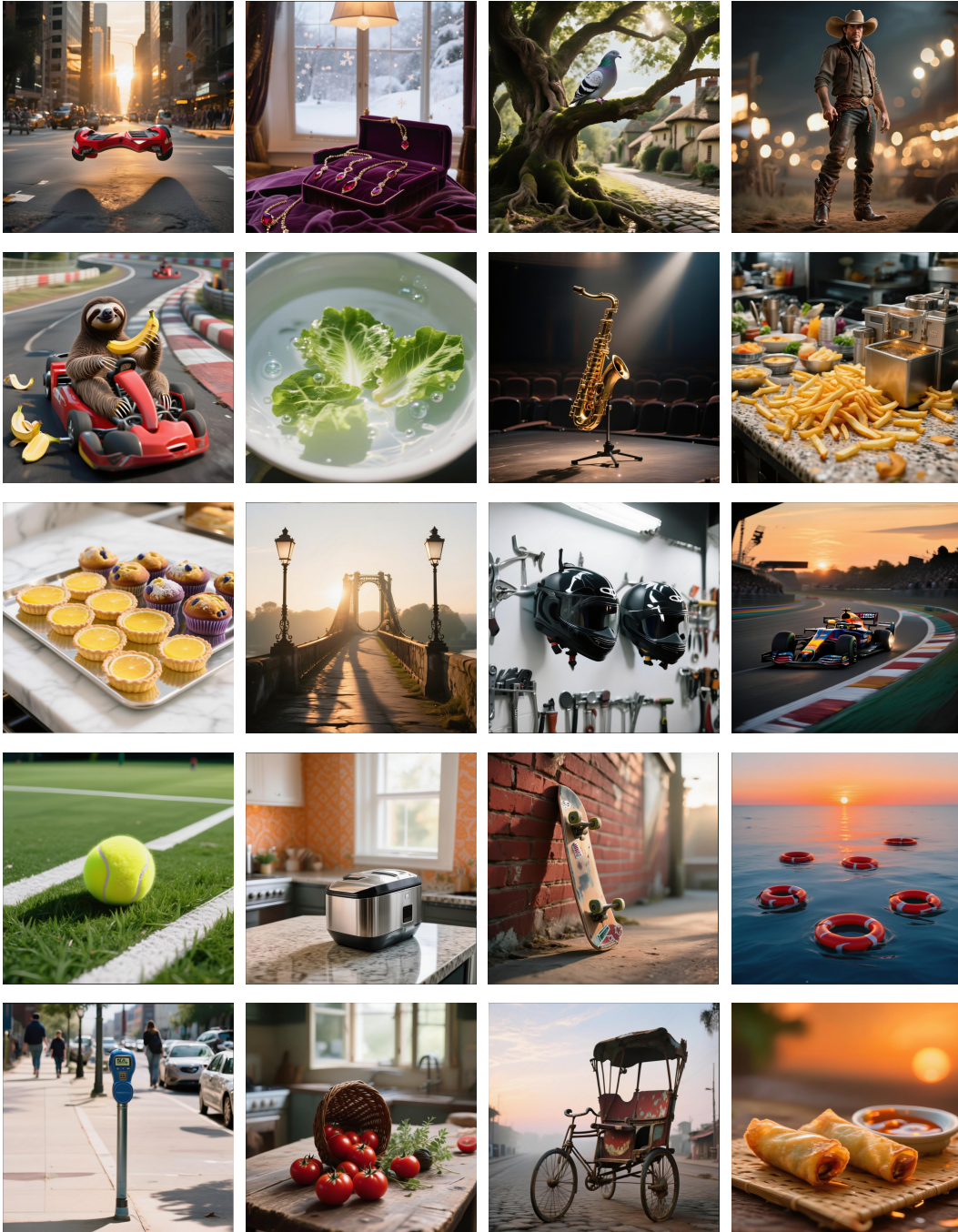


Figure 5: More qualitative results on text-to-image generation

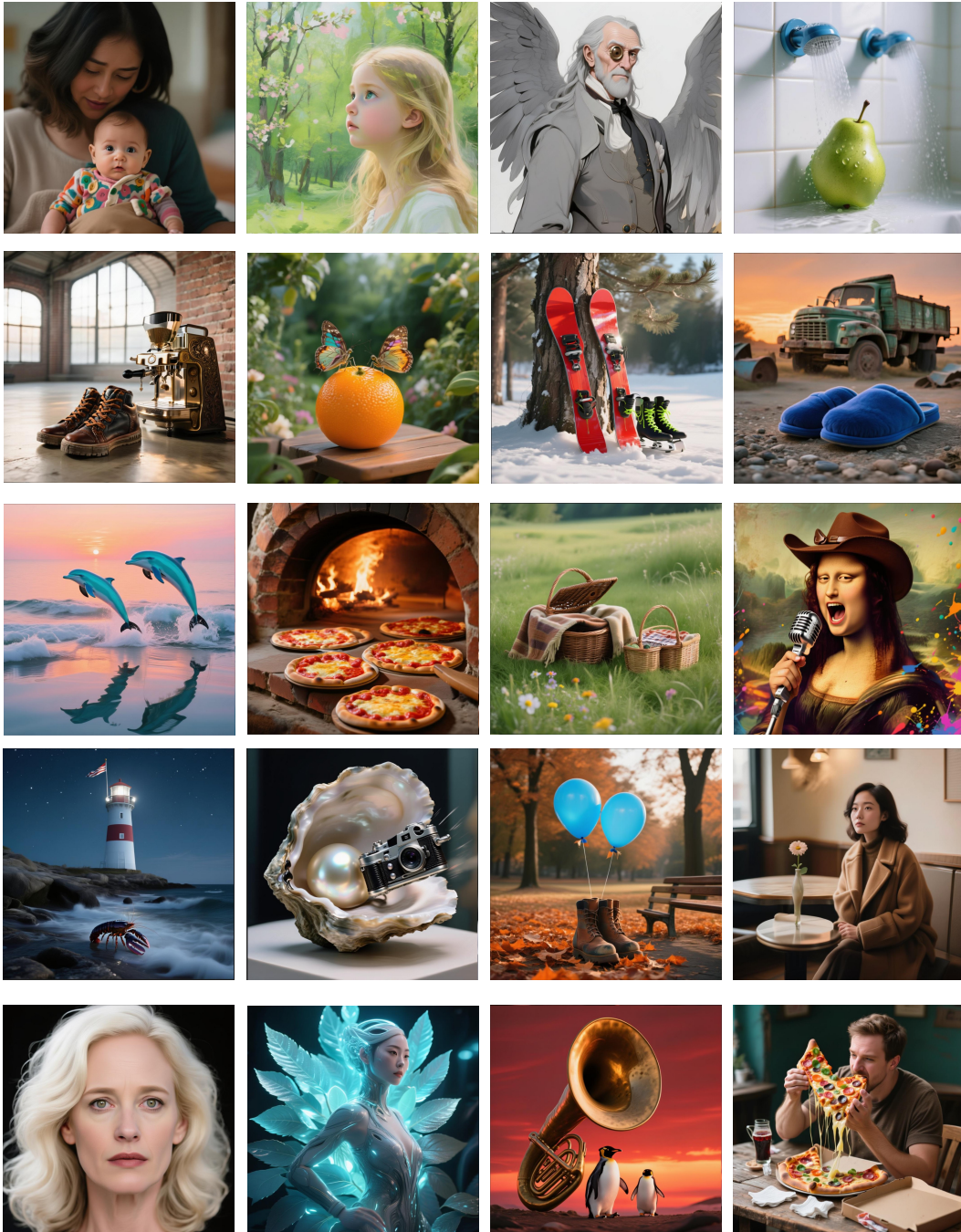


Figure 6: More qualitative results on text-to-image generation



Add a vintage car driving along the dirt path in the foreground of the image.



Add a coffee mug on the table in the foreground.



Add a small wooden cabin with a chimney near the edge of the forest on the right side of the image.



Add a person walking in the foreground near the broken wooden fence, dressed in winter clothing.



Change the stage background to a beach setting with palm trees and the ocean visible in the distance.



Replace the rocky background with a lush green forest setting, while keeping the mountain goat.



Change the background from the ocean to an urban cityscape with the yacht cruising down a river.



Extract the animal in the image, including its full body and fur details.



Remove the human child bending over the.



Remove the rainbow paint and spot from the face.

Figure 7: More qualitative results on image editing